

A Rigorous Mathematical Theory for Topological Phases and Edge Modes in Spring-mass Mechanical Systems

Ridvan Ozdemir ^{*} and Junshan Lin [†]

Abstract

In this work, we examine the topological phases of the spring-mass lattices when the spatial inversion symmetry of the system is broken and prove the existence of edge modes when two lattices with different topological phases are glued together. In particular, for the one-dimensional lattice consisting of an infinite array of masses connected by springs, we show that the Zak phase of the lattice is quantized, only taking the value 0 or π . We also prove the existence of an edge mode when two semi-infinite lattices with distinct Zak phases are connected. For the two-dimensional honeycomb lattice, we characterize the valley Chern numbers of the lattice when the masses on the lattice vertices are uneven. The existence of edge modes is proved for a joint honeycomb lattice formed by gluing two semi-infinite lattices with opposite valley Chern numbers together.

1 Introduction

The recent development of topological insulators in condensed matter physics has opened up new avenues for localization and confinement of classical waves. In topological insulators, an insulating bulk electronic material can support localized edge states on its surface, and the existence of edge states is associated with the topological invariant of the bulk electron material [1]. The extension of concepts in topological insulators to classical waves was proposed in the seminal work [2], where the topological phases in the electromagnetic wave systems were introduced using the wave functions in the momentum space. Since then extensive research has been devoted to control acoustic, electromagnetic and mechanical waves in the same way as solids modulating electrons in topological insulators [3–7].

There exist mainly two strategies to realize topological wave insulators for classical waves. The first strategy mimics the so-called quantum Hall effect in topological insulator using active components to break the time-reversal symmetry of the system. This is realized by moderating rotational motion of air in acoustic media or applying the external magnetic field in electromagnetic media [8–10]. The second strategy relies on an analogue of the quantum spin Hall effect or quantum valley Hall effect, and it uses passive components to break the inversion symmetry of the system [11–14]. In this work, we investigate the spring-mass topological mechanical systems using the second strategy. The inversion symmetry in each periodic cell of the system is broken by tuning either the mass parameter or the spring constant. The setup of the topological mechanical material was introduced in [15], and our goal in this work is to provide a rigorous mathematical theory for the topological phases and edge modes in such mechanical systems. The spring-mass topological mechanical systems using the first strategy was realized in [16]. The mathematical studies for the corresponding topological phases and edge modes will be forthcoming.

We examine topological mechanical systems in one and two dimensions. The periodic lattice in one dimension is constructed over the real line with identical masses, wherein each mass is connected by two springs with different spring constants. We derive the Zak phase of the lattice and show that its value is quantized when the spring constant varies, only taking the value 0 or π . Additionally, we prove the existence of edge modes when two semi-infinite mechanical systems with different Zak phases are joined together. In two dimensions, the periodic mechanical system is constructed over a honeycomb lattice, wherein each

^{*}Department of Mathematics and Statistics, Auburn University, Auburn, AL 36849. rzo0012@auburn.edu.

[†]Department of Mathematics and Statistics, Auburn University, Auburn, AL 36849. jz10097@auburn.edu.

periodic cell consists of two different masses that are connected to the neighboring masses with the identical springs. We investigate the valley Chern number and examine how its value is related to the change of masses. Furthermore, we prove the existence of the edge modes in a joint mechanical system formed by two honeycomb lattices with opposite valley Chern numbers. We would like to refer the readers to the mathematical studies of edge modes in acoustic and electromagnetic waves in [17–23]. In general, the number of edge modes is equal to the difference of the bulk topological invariants across the interface, which is known as the bulk-edge correspondence. We refer to [24–28] for the bulk-edge correspondence in electron models for topological insulators and several elliptic partial differential equation models.

The rest of the paper is organized as follows. In Section 2, we consider the one-dimensional spring-mass mechanical system. The Zak phase of the lattice is given in Lemma 2 and the existence of the edge modes for the joint lattice is established in Theorem 1. In Section 3, we investigate the two-dimensional mechanical system over the honeycomb lattice. The valley Chern number for the lattice is summarized in Lemma 3 when the masses on the lattice vertices are uneven. Finally, the existence of edge modes for the joint topological mechanical insulator is established in Theorem 2.

2 One-dimensional Topological Mechanical Systems

2.1 Periodic Mechanical System

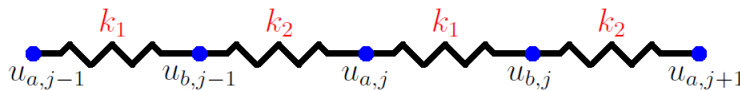


Figure 1: One-dimensional lattice consisting of an array of masses connected by springs.

We consider the one-dimensional periodic mechanical system shown in Figure 1, wherein an infinite array of masses are arranged along real line. The spring connecting two masses in the unit cell j and two masses between the cell j and $j + 1$ attains the spring constants

$$k_1 = k(1 + \gamma) \text{ and } k_2 = k(1 - \gamma), \quad (1)$$

where γ is a stiffness parameter and k is the mean stiffness of the springs. The displacements of masses in the unit cell j satisfies the following equations:

$$\begin{aligned} mU''_{a,j} + k_1(U_{a,j} - U_{b,j}) + k_2(U_{a,j} - U_{b,j-1}) &= 0, \\ mU''_{b,j} + k_2(U_{b,j} - U_{a,j+1}) + k_1(U_{b,j} - U_{a,j}) &= 0. \end{aligned}$$

We consider the solution in the form of

$$U_{a,j}(t) = u_a e^{i\omega\tau + \mu j} \text{ and } U_{b,j}(t) = u_b e^{i\omega\tau + \mu j} \quad (2)$$

where u_a and u_b are the amplitudes of the displacements of masses, j denotes the cell index, ω is the frequency, $\tau = \sqrt{k/mt}$ is nondimensional time scale and $\mu \in [-\pi, \pi]$ is the nondimensional wave number. Then u_a and u_b satisfy

$$\begin{aligned} -m\frac{k}{m}\omega^2 u_a + k(1 + \gamma)(u_a - u_b)e^{i\omega\tau + \mu j} + k(1 - \gamma)(u_a - u_b e^{-i\mu})e^{i\omega\tau + \mu j} &= 0, \\ -m\frac{k}{m}\omega^2 u_b + k(1 + \gamma)(u_b - u_a e^{i\mu})e^{i\omega\tau + \mu j} + k(1 - \gamma)(u_b - u_a)e^{i\omega\tau + \mu j} &= 0, \end{aligned}$$

which reduces to the eigenvalue problem

$$\begin{bmatrix} 2 & \bar{a}(\mu) \\ a(\mu) & 2 \end{bmatrix} \begin{bmatrix} u_a \\ u_b \end{bmatrix} = \omega^2 \begin{bmatrix} u_a \\ u_b \end{bmatrix}, \quad (3)$$

where $a(\mu) = -(1 + \gamma) - (1 - \gamma)e^{i\mu}$ and $\bar{a}(\mu)$ is the complex conjugate of $a(\mu)$. The eigenpairs of matrix in (3) are

$$\lambda_{\pm}(\mu) = 2 \pm |a(\mu)| \quad \text{and} \quad \mathbf{v}_{\pm}(\mu) = \frac{1}{\sqrt{2}} \begin{bmatrix} \frac{\bar{a}(\mu)}{\mp |a(\mu)|} \\ 1 \end{bmatrix},$$

with $\|\mathbf{v}_{\pm}(\mu)\|_2 = 1$. We note that if $\gamma \neq 0$, then $|a(\mu)| \neq 0$ and there is a gap between two bands $\lambda_-(\mu)$ and $\lambda_+(\mu)$ for $\mu \in [-\pi, \pi]$. We call this gap as the band gap interval

$$I(\gamma) := (\sqrt{2(1 - |\gamma|)}, \sqrt{2(1 + |\gamma|)}), \quad (4)$$

where $\sqrt{2(1 - |\gamma|)}$ and $\sqrt{2(1 + |\gamma|)}$ are maximum and minimum values of $\sqrt{\lambda_-(\mu)}$ and $\sqrt{\lambda_+(\mu)}$ respectively. We investigate the dynamics of the system for the frequency ω located in the band gap $I(\gamma)$ which is induced by a topological index called Zak phase.

The Zak phase associated with the frequency band $\lambda(\mu)$ is defined by (cf. [29])

$$\theta^{Zak} = \int_{-\pi}^{\pi} \left[i (\mathbf{v}(\mu))^H \partial_{\mu} \mathbf{v}(\mu) \right] d\mu = -Im \left(\int_{-\pi}^{\pi} \left[(\mathbf{v}(\mu))^H \partial_{\mu} \mathbf{v}(\mu) \right] d\mu \right), \quad (5)$$

where $\mathbf{v} = \mathbf{v}_+$ or $\mathbf{v} = \mathbf{v}_-$ is the eigenvector associated with the eigenvalue $\lambda_{\pm}(\mu)$ of the matrix defined in (3) and \mathbf{v}^H stands for complex conjugate transpose of \mathbf{v} . To avoid the difficulties in calculation of the composition of differentiation and integration, we use the discretization of the integral in (5). To this purpose, for $\mu_n = n\pi/N$, $n = -N, -(N-1), \dots, N-1, N$ where $N \in \mathbb{Z}^+$, we observe that

$$\begin{aligned} \log \left[(\mathbf{v}(\mu_n))^H \mathbf{v}(\mu_{n+1}) \right] &= \log \left[(\mathbf{v}(\mu_n))^H (\mathbf{v}(\mu_n) + \partial_{\mu} \mathbf{v}(\mu_n)(\mu_{n+1} - \mu_n)) + O(N^{-2}) \right] \\ &= \log \left[(\mathbf{v}(\mu_n))^H \mathbf{v}(\mu_n) + (\mathbf{v}(\mu_n))^H \partial_{\mu} \mathbf{v}(\mu_n)(\mu_{n+1} - \mu_n) + O(N^{-2}) \right] \\ &= \log \left[1 + (\mathbf{v}(\mu_n))^H \partial_{\mu} \mathbf{v}(\mu_n)(\mu_{n+1} - \mu_n) + O(N^{-2}) \right] \\ &= (\mathbf{v}(\mu_n))^H \partial_{\mu} \mathbf{v}(\mu_n)(\mu_{n+1} - \mu_n) + O(N^{-2}). \end{aligned}$$

Then, by discretization of the integral, Zak phase can be written as

$$\begin{aligned} \theta^{Zak} &= -Im \left(\int_{-\pi}^{\pi} \left[(\mathbf{v}(\mu))^H \partial_{\mu} \mathbf{v}(\mu) \right] d\mu \right) \\ &= -Im \left(\lim_{N \rightarrow \infty} \sum_{n=-N}^{N-1} (\mathbf{v}(\mu_n))^H \partial_{\mu} \mathbf{v}(\mu_n)(\mu_{n+1} - \mu_n) \right) \\ &= \lim_{N \rightarrow \infty} - \sum_{n=-N}^{N-1} Im \left(\log \left[(\mathbf{v}(\mu_n))^H \mathbf{v}(\mu_{n+1}) \right] \right). \end{aligned}$$

We define the discrete Zak Phase as

$$\theta_N^{Zak} := - \sum_{n=-N}^{N-1} Im \left(\log \left[(\mathbf{v}(\mu_n))^H \mathbf{v}(\mu_{n+1}) \right] \right).$$

We have the following lemma for a complex number:

Lemma 1. For a complex number $z = re^{i\theta}$ with $\theta \in [-\pi, \pi]$, if $z + 1 = |z + 1|e^{i\beta}$, there holds

$$\begin{cases} \beta < \theta/2, & \text{for } r < 1, \\ \beta = \theta/2, & \text{for } r = 1, \\ \beta > \theta/2, & \text{for } r > 1. \end{cases}$$

Proof. For $z = a + ib$, the half angle formula gives that

$$\tan(\theta/2) = \frac{\sin(\theta)}{1 + \cos(\theta)} = \frac{b/r}{1 + a/r} = \frac{b}{r + a}.$$

Also, since $\tan(\beta) = \frac{b}{1+a}$, the results follow by the fact that tangent is an increasing function on $[-\pi, \pi]$. \square

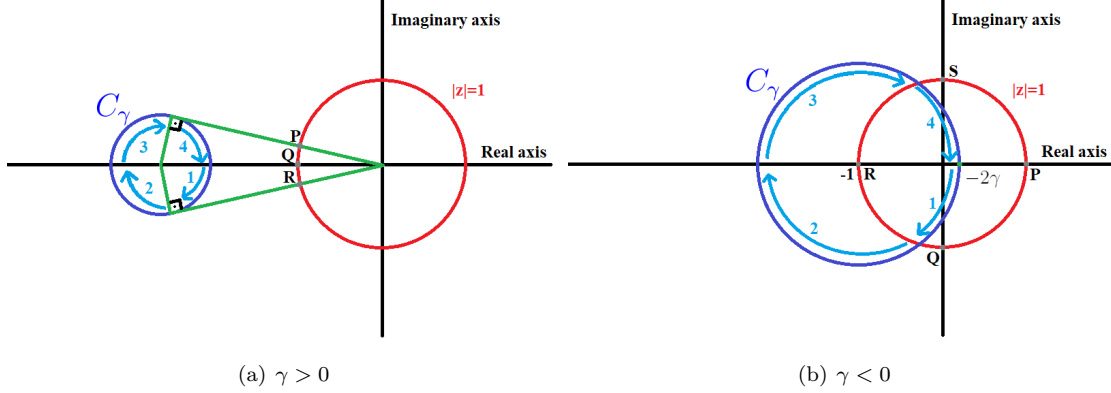


Figure 2: When $\gamma > 0$, C_γ , the circle with center $-(1 + \gamma)$ and radius $1 - \gamma$, does not enclose the origin. As $a(\mu)$ completes one turn on C_γ from 1 to 4, the trajectory of $\frac{a(\mu)}{|a(\mu)|}$ is the path $Q \rightarrow R \rightarrow Q \rightarrow P \rightarrow Q$ on the unit circle and its argument oscillates near π . When $\gamma < 0$, C_γ contains origin. As $a(\mu)$ completes one turn on C_γ , the trajectory of $\frac{a(\mu)}{|a(\mu)|}$ is the path $P \rightarrow Q \rightarrow R \rightarrow S \rightarrow P$ on the unit circle and its argument goes from 2π to 0.

Lemma 2. For the Zak phase θ^{Zak} associated with the band $\lambda_-(\mu)$ or $\lambda_+(\mu)$ of the system (3), we have

$$\begin{cases} \theta^{Zak} = 0, & \text{if } \gamma > 0, \\ \theta^{Zak} = \pi, & \text{if } \gamma < 0. \end{cases}$$

Proof. For $\lambda_+(\mu)$, we have $\mathbf{v} = \mathbf{v}_+$. Let θ_n be the argument of the first component of $\mathbf{v}_+(\mu_n)$. Then a direct computation leads to

$$\begin{aligned} \mathbf{v}_+^H(\mu_n) \mathbf{v}_+(\mu_{n+1}) &= \frac{1}{2} \left(\begin{bmatrix} \frac{a(\mu_n)}{|a(\mu_n)|} & 1 \\ \frac{\bar{a}(\mu_{n+1})}{|a(\mu_{n+1})|} & 1 \end{bmatrix} \right) \\ &= \frac{1}{2} \left(e^{i(\theta_{n+1} - \theta_n)} + 1 \right) \\ &= \frac{c_n}{2} \exp\left(i \frac{\theta_{n+1} - \theta_n}{2}\right), \end{aligned}$$

where c_n is the modulus of $e^{i(\theta_{n+1} - \theta_n)} + 1$ and we have used Lemma 1 in the last step. Thus the discrete Zak phase

$$\begin{aligned} \theta_N^{Zak} &= - \sum_{n=-N}^{N-1} \text{Im} \left(\log [\mathbf{v}_+^H(\mu_n) \mathbf{v}_+(\mu_{n+1})] \right) = - \sum_{n=-N}^{N-1} \text{Im} \left(\log \left[\frac{c_n}{2} \left(\exp\left(i \frac{\theta_{n+1} - \theta_n}{2}\right) \right) \right] \right) \\ &= - \frac{\theta_N - \theta_{-N}}{2}. \end{aligned}$$

If $\gamma > 0$, we denote the circle with center $-(1 + \gamma)$ and radius $1 - \gamma$ as C_γ . As μ goes from $-\pi$ to π , $\bar{a}(\mu) = -(1 + \gamma) - (1 - \gamma)e^{-i\mu}$ completes one turn on the circle C_γ clockwise starting from the point -2γ on complex plane. Since $|(1 + \gamma)| = 1 + \gamma > 1 - \gamma$, the distance between the center of C_γ and the origin is greater than its radius, hence C_γ does not enclose the origin (see Figure 2(a)). Therefore, the argument of $\frac{a(\mu)}{|a(\mu)|}$ oscillates around π as μ goes from $-\pi$ to π . As a result, we obtain $\theta_N = \theta_{-N}$ and

$$\theta_N^{Zak} = -\frac{\theta_N - \theta_{-N}}{2} = 0.$$

If $\gamma < 0$, $\bar{a}(\mu)$ still completes one turn on the circle C_γ . However, noting that the distance between the center of C_γ and the origin is less than the radius of C_γ and C_γ encloses the origin. Thus the argument of $\frac{a(\mu)}{|a(\mu)|}$ goes from 2π to 0 (see Figure 2(b)) and we have

$$\theta_N^{Zak} = -\frac{\theta_N - \theta_{-N}}{2} = -\frac{0 - 2\pi}{2} = \pi.$$

For $\lambda_-(\mu)$, we can obtain the same results by similar calculations. Therefore, the proof is complete by noting that $\theta^{Zak} = \lim_{N \rightarrow \infty} \theta_N^{Zak}$. \square

2.2 Edge Modes for the Topological Mechanical System

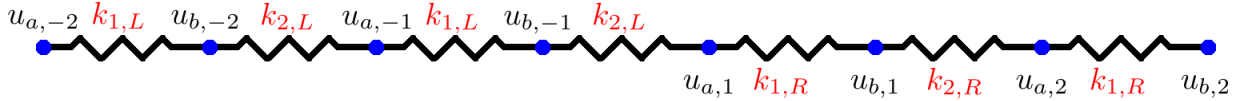


Figure 3: The topological mechanical system in one dimension

We construct a joint system by gluing two periodic mechanical systems with different spring constants as shown in Figure 3. On the left, the spring constants defined in (1) for each unit cell are $k_{1,L} = k(1 + \gamma_L)$, $k_{2,L} = k(1 - \gamma_L)$ and the spring constants for each unit cell on the right are $k_{1,R} = k(1 + \gamma_R)$ and $k_{2,R} = k(1 - \gamma_R)$. We assume that γ_L and γ_R have different signs. In the light of Lemma 2, these two systems attain different Zak phases, $\theta_L \neq \theta_R$. For $j = 2, 3, \dots$, the governing equations for the displacement of the masses at the left and right periodic systems are

$$\begin{aligned} mU_{a,-j+1}'' + k_{1,L}(U_{a,-j+1} - U_{b,-j+1}) + k_{2,L}(U_{a,-j+1} - U_{b,-j}) &= 0, \\ mU_{b,-j}'' + k_{2,L}(U_{b,-j} - U_{a,-j+1}) + k_{1,L}(U_{b,-j} - U_{a,-j}) &= 0, \end{aligned} \quad (6)$$

and

$$\begin{aligned} mU_{a,j}'' + k_{1,R}(U_{a,j} - U_{b,j}) + k_{2,R}(U_{a,j} - U_{b,j-1}) &= 0, \\ mU_{b,j-1}'' + k_{2,R}(U_{b,j-1} - U_{a,j}) + k_{1,R}(U_{b,j-1} - U_{a,j-1}) &= 0. \end{aligned} \quad (7)$$

respectively. The governing equations for the displacement of the masses located at the interface of two periodic systems are

$$\begin{aligned} mU_{a,1}'' + k_{1,R}(U_{a,1} - U_{b,1}) + k_{2,L}(U_{a,1} - U_{b,-1}) &= 0, \\ mU_{b,-1}'' + k_{2,L}(U_{b,-1} - U_{a,1}) + k_{1,L}(U_{b,-1} - U_{a,-1}) &= 0. \end{aligned} \quad (8)$$

A non-trivial solution $(U_{a,j}(t), U_{b,j}(t))$ for (6) - (8) which decays to zero as $j \rightarrow \pm\infty$ is called an edge mode.

In the rest of this subsection, we aim to show the existence of edge modes for the joint system in Figure 3 when $\theta_L \neq \theta_R$ and $\omega \in I$, the common band gap, where

$$I := I(\gamma_R) \cap I(\gamma_L) = \left[\sqrt{2(1 - |\gamma_R|)}, \sqrt{2(1 + |\gamma_R|)} \right] \cap \left[\sqrt{2(1 - |\gamma_L|)}, \sqrt{2(1 + |\gamma_L|)} \right].$$

Our main result is stated in the following theorem:

Theorem 1. (Existence of edge modes) If $\gamma_L\gamma_R < 0$ such that two periodic mechanical systems with the Zak phase $\theta_L \neq \theta_R$ are glued together as shown in Figure 3, then there exists an edge mode $(U_{a,j}(t), U_{b,j}(t))$ in the form of

$$U_{a,j}(t) = u_{a,j}e^{i\omega\tau} \text{ and } U_{b,j}(t) = u_{b,j}e^{i\omega\tau} \quad (9)$$

where j denotes the cell index, τ is the nondimensional time scale and $\omega \in I$.

2.2.1 Transfer Matrix for the Periodic System

Assume that the solutions of (6)-(7) take the form in (9). For the right periodic system, $u_{a,j}$ and $u_{b,j}$ satisfy

$$\begin{aligned} -m\frac{k}{m}\omega^2 u_{a,j}e^{i\omega\tau} + k(1+\gamma_R)(u_{a,j}e^{i\omega\tau} - u_{b,j}e^{i\omega\tau}) + k(1-\gamma_R)(u_{a,j}e^{i\omega\tau} - u_{b,j-1}e^{i\omega\tau}) &= 0, \\ -m\frac{k}{m}\omega^2 u_{b,j-1}e^{i\omega\tau} + k(1-\gamma_R)(u_{b,j-1}e^{i\omega\tau} - u_{a,j}e^{i\omega\tau}) + k(1+\gamma_R)(u_{b,j-1}e^{i\omega\tau} - u_{a,j-1}e^{i\omega\tau}) &= 0, \end{aligned}$$

which implies

$$\begin{aligned} (2-\omega^2)u_{a,j} - (1+\gamma_R)u_{b,j} - (1-\gamma_R)u_{b,j-1} &= 0, \\ (2-\omega^2)u_{b,j-1} - (1-\gamma_R)u_{a,j} - (1+\gamma_R)u_{a,j-1} &= 0. \end{aligned}$$

This can be written as the system $A\mathbf{u}_{j-1} = B\mathbf{u}_j$, where

$$A = \begin{bmatrix} 0 & 1-\gamma_R \\ -(1+\gamma_R) & 2-\omega^2 \end{bmatrix}, \quad B = \begin{bmatrix} 2-\omega^2 & -(1+\gamma_R) \\ 1-\gamma_R & 0 \end{bmatrix} \text{ and } \mathbf{u}_j = \begin{bmatrix} u_{a,j} \\ u_{b,j} \end{bmatrix}.$$

We rewrite $A\mathbf{u}_{j-1} = B\mathbf{u}_j$ as

$$T_R\mathbf{u}_{j-1} = \mathbf{u}_j,$$

where the transfer matrix

$$T_R = B^{-1}A = \begin{bmatrix} -\frac{1+\gamma_R}{1-\gamma_R} & \frac{2-\omega^2}{1-\gamma_R} \\ -\frac{2-\omega^2}{1-\gamma_R} & \frac{(2-\omega^2)^2 - (1-\gamma_R)^2}{1-\gamma_R^2} \end{bmatrix}.$$

It can be shown that

$$\det(T_R) = 1.$$

The eigenvalues of T_R are

$$\begin{aligned} \lambda_{\pm,R} &= \frac{1}{2} \left(\frac{(2-\omega^2)^2 - (1-\gamma_R)^2 - (1+\gamma_R)^2}{1-\gamma_R^2} \pm \sqrt{\frac{1}{(1-\gamma_R^2)^2} [\omega^4 - 4\omega^2] [(2-\omega^2)^2 - 4\gamma_R^2]} \right) \\ &= \frac{1}{2(1-\gamma_R^2)} \left((2-\omega^2)^2 - (1-\gamma_R)^2 - (1+\gamma_R)^2 \pm \sqrt{\omega^2(\omega^2-4) [(2-\omega^2)^2 - 4\gamma_R^2]} \right). \end{aligned}$$

The corresponding eigenvectors $\mathbf{e}_{\pm,R}$ are

$$\mathbf{e}_{\pm,R} = \begin{bmatrix} (2-\omega^2) \\ 1+\gamma_R + (1-\gamma_R)\lambda_{\pm,R} \end{bmatrix}. \quad (10)$$

For the left periodic system, similar calculations give that

$$T_L\mathbf{u}_{-j+1} = \mathbf{u}_{-j}$$

where the transfer matrix

$$T_L = \begin{bmatrix} \frac{(2-\omega^2)^2 - (1-\gamma_L)^2}{1-\gamma_L^2} & -\frac{2-\omega^2}{1-\gamma_L} \\ \frac{2-\omega^2}{1-\gamma_L} & \frac{1+\gamma_L}{1-\gamma_L} \end{bmatrix},$$

with eigenvalues

$$\lambda_{\pm,L} := \frac{1}{2(1-\gamma_L^2)} \left((2-\omega^2)^2 - (1-\gamma_L)^2 - (1+\gamma_L)^2 \pm \sqrt{\omega^2(\omega^2-4) \left[(2-\omega^2)^2 - 4\gamma_L^2 \right]} \right)$$

and the corresponding eigenvector

$$\mathbf{e}_{\pm,L} = \begin{bmatrix} 1 + \gamma_L + (1-\gamma_L)\lambda_{\pm,L} \\ 2-\omega^2 \end{bmatrix}.$$

Note that $\sqrt{2(1-|\gamma_L|)} < \sqrt{2(1+|\gamma_R|)} \leq \sqrt{2(1+|\gamma_L|)}$ and $\sqrt{2(1-|\gamma_R|)} < \sqrt{2(1+|\gamma_L|)} \leq \sqrt{2(1+|\gamma_R|)}$ when $|\gamma_R| \leq |\gamma_L|$ and $|\gamma_L| \leq |\gamma_R|$ respectively. It follows that $I \neq \emptyset$.

For $\omega \in I$, $\lambda_{\pm,R}$ and $\lambda_{\pm,L}$ are real. Since $\det(T_R) = 1$ and $\lambda_{+,R} \neq \lambda_{-,R}$, one of $|\lambda_{+,R}|$ and $|\lambda_{-,R}|$ is less than 1, $\mathbf{e}_{+,R}$ and $\mathbf{e}_{-,R}$ are linearly independent and $\{\mathbf{e}_{+,R}, \mathbf{e}_{-,R}\}$ form a basis of \mathbb{R}^2 . Hence, $\mathbf{u}_1 = \begin{bmatrix} u_{a,1} \\ u_{b,1} \end{bmatrix}$ can be written as

$$\mathbf{u}_1 = a_1 \mathbf{e}_{+,R} + a_2 \mathbf{e}_{-,R}$$

for some constants $a_1, a_2 \in \mathbb{R}$. Then

$$\mathbf{u}_j = T_R^j \mathbf{u}_1 = a_1 (\lambda_{+,R})^{j-1} \mathbf{e}_{+,R} + a_2 (\lambda_{-,R})^{j-1} \mathbf{e}_{-,R}.$$

For \mathbf{u}_j to vanish as $j \rightarrow \infty$, it is necessary that $\mathbf{u}_1 = \begin{bmatrix} u_{a,1} \\ u_{b,1} \end{bmatrix}$ is parallel to the eigenvector of T_R whose corresponding eigenvalue has absolute value less than 1. Similarly, $\mathbf{u}_{-1} = \begin{bmatrix} u_{a,-1} \\ u_{b,-1} \end{bmatrix}$ must be parallel to the eigenvector of T_L whose corresponding eigenvalue has absolute value less than 1 in order for \mathbf{u}_j to vanish as $j \rightarrow -\infty$.

To find the eigenvalues of T_R and T_L with absolute value less than 1, we have

$$\begin{aligned} (2-\omega^2)^2 - (1-\gamma_R)^2 - (1+\gamma_R)^2 &\leq (2\min\{|\gamma_R|, |\gamma_L|\})^2 - (1-\gamma_R)^2 - (1+\gamma_R)^2 \\ &\leq 4\gamma_R^2 - 1 + 2\gamma_R - \gamma_R^2 - 1 - 2\gamma_R - \gamma_R^2 \\ &= 2(\gamma_R^2 - 1) \leq 0. \end{aligned}$$

Thus $\lambda_-(\gamma_R) < \lambda_+(\gamma_L) < 0$ and the eigenvalue of T_R with absolute value less than 1 is

$$\lambda_R := \lambda_{+,R} = \frac{1}{2(1-\gamma_R^2)} \left((2-\omega^2)^2 - (1-\gamma_R)^2 - (1+\gamma_R)^2 + \omega \sqrt{(\omega^2-4) \left[(2-\omega^2)^2 - 4\gamma_R^2 \right]} \right).$$

The corresponding eigenvector \mathbf{e}_R is

$$\mathbf{e}_R := \mathbf{e}_{+,R} = \begin{bmatrix} (2-\omega^2) \\ 1 + \gamma_R + (1-\gamma_R)\lambda_R \end{bmatrix}. \quad (11)$$

By similar calculations, we obtain

$$\lambda_L := \frac{1}{2(1-\gamma_L^2)} \left((2-\omega^2)^2 - (1-\gamma_L)^2 - (1+\gamma_L)^2 + \omega \sqrt{(\omega^2-4) \left[(2-\omega^2)^2 - 4\gamma_L^2 \right]} \right)$$

and the corresponding eigenvector

$$\mathbf{e}_L = \begin{bmatrix} 1 + \gamma_L + (1 - \gamma_L) \lambda_L \\ 2 - \omega^2 \end{bmatrix}. \quad (12)$$

Therefore, we obtain that $\mathbf{u}_1 = \begin{bmatrix} u_{a,1} \\ u_{b,1} \end{bmatrix}$ must be parallel to \mathbf{e}_R and $\mathbf{u}_{-1} = \begin{bmatrix} u_{a,-1} \\ u_{b,-1} \end{bmatrix}$ must be parallel to \mathbf{e}_L to vanish as $j \rightarrow \pm\infty$.

2.2.2 Proof of Theorem 1

By substituting (9) into the equations (8), we get

$$\begin{aligned} (2 - \omega^2 + \gamma_R - \gamma_L) u_{a,1} - (1 + \gamma_R) u_{b,1} - (1 - \gamma_L) u_{b,-1} &= 0, \\ (2 - \omega^2) u_{b,-1} - (1 - \gamma_L) u_{a,1} - (1 + \gamma_L) u_{a,-1} &= 0. \end{aligned} \quad (13)$$

Since $\begin{bmatrix} u_{a,1} \\ u_{b,1} \end{bmatrix}$ and $\begin{bmatrix} u_{a,-1} \\ u_{b,-1} \end{bmatrix}$ are parallel to \mathbf{e}_R and \mathbf{e}_L respectively, there holds

$$\begin{bmatrix} u_{a,1} \\ u_{b,1} \end{bmatrix} = c_1 \mathbf{e}_R \text{ and } \begin{bmatrix} u_{a,-1} \\ u_{b,-1} \end{bmatrix} = c_2 \mathbf{e}_L$$

for some constants c_1 and c_2 . Then by (13), we obtain

$$\begin{aligned} (2 - \omega^2 + \gamma_R - \gamma_L) c_1 (2 - \omega^2) - (1 + \gamma_R) c_1 (1 + \gamma_R + (1 - \gamma_R) \lambda_R) - (1 - \gamma_L) c_2 (2 - \omega^2) &= 0, \\ (2 - \omega^2) c_2 (2 - \omega^2) - (1 - \gamma_L) c_1 (2 - \omega^2) - (1 + \gamma_L) c_2 (1 + \gamma_L + (1 - \gamma_L) \lambda_L) &= 0. \end{aligned} \quad (14)$$

(14) can be simplified as

$$\begin{aligned} \left[\Omega^2 + (\gamma_R - \gamma_L) \Omega - (1 + \gamma_R)^2 - (1 - \gamma_R^2) \lambda_R \right] c_1 &= (1 - \gamma_L) \Omega c_2, \\ \left[\Omega^2 - (1 + \gamma_L)^2 - (1 - \gamma_L^2) \lambda_L \right] c_2 &= (1 - \gamma_L) \Omega c_1, \end{aligned} \quad (15)$$

where $\Omega = 2 - \omega^2$. Multiplying the second equation in (15) by $(1 - \gamma_L) \Omega$ gives

$$\left[\Omega^2 - (1 + \gamma_L)^2 - (1 - \gamma_L^2) \lambda_L \right] (1 - \gamma_L) \Omega c_2 = (1 - \gamma_L)^2 \Omega^2 c_1. \quad (16)$$

By the first equation in (15) and (16), we have

$$\left[\Omega^2 - (1 + \gamma_L)^2 - (1 - \gamma_L^2) \lambda_L \right] \left[\Omega^2 + (\gamma_R - \gamma_L) \Omega - (1 + \gamma_R)^2 - (1 - \gamma_R^2) \lambda_R \right] = (1 - \gamma_L)^2 \Omega^2,$$

which can be simplified as

$$\left[\Omega^2 - 4\gamma_L - \sqrt{(4 - \Omega^2)(4\gamma_L^2 - \Omega^2)} \right] \left[\Omega^2 + 2(\gamma_R - \gamma_L) \Omega - 4\gamma_R - \sqrt{(4 - \Omega^2)(4\gamma_R^2 - \Omega^2)} \right] = 4(1 - \gamma_L)^2 \Omega^2. \quad (17)$$

Observe that, for $\Omega = 0$, we have

$$\left[0^2 - 4\gamma_L - \sqrt{(4 - 0^2)(4\gamma_L^2 - 0^2)} \right] \left[0^2 + 2(\gamma_R - \gamma_L) 0 - 4\gamma_R - \sqrt{(4 - 0^2)(4\gamma_R^2 - 0^2)} \right] = 4(1 - \gamma_L)^2 0^2$$

which is equivalent to

$$(\gamma_L + |\gamma_L|)(\gamma_R + |\gamma_R|) = 0. \quad (18)$$

Since γ_L and γ_R have different signs, either $\gamma_L + |\gamma_L| = 0$ or $\gamma_R + |\gamma_R| = 0$. Therefore, (18) holds and $\Omega = 0$ is a solution of (17). Note that $\Omega = 0$ gives $\omega = \sqrt{2} \in I$. This proves the theorem.

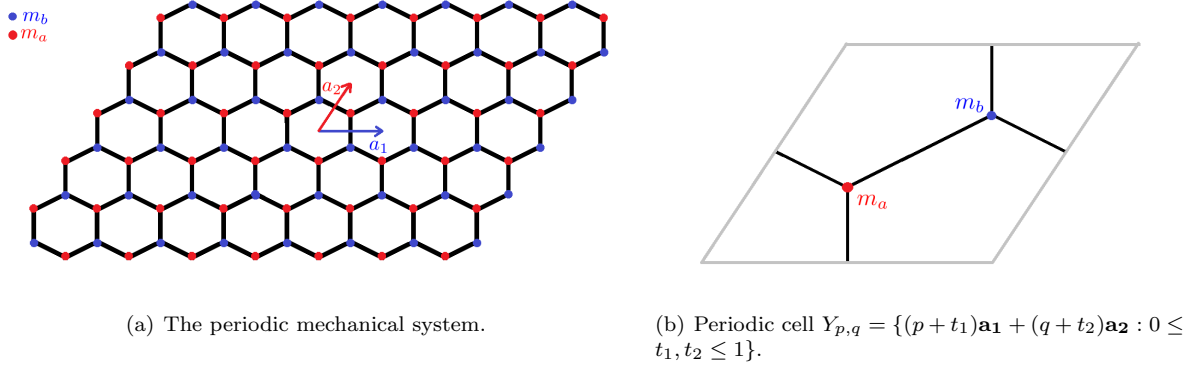


Figure 4: The periodic mechanical system over the honeycomb lattice.

3 Two-dimensional Honeycomb Topological Mechanical System

3.1 Periodic Mechanical System

3.1.1 Mathematical Model

We consider the two-dimensional mechanical system over the honeycomb lattice as shown in Figure 4(a). Let $\mathbf{a}_1 = a[1, 0]$ and $\mathbf{a}_2 = a[\frac{1}{2}, \frac{\sqrt{3}}{2}]$ be the lattice vectors where a is the lattice constant. Then the honeycomb lattice is given by $\Lambda := \sum_{p,q \in \mathbb{Z}} Y_{p,q}$, where $Y_{p,q} = \{(p+t_1)\mathbf{a}_1 + (q+t_2)\mathbf{a}_2 : 0 \leq t_1, t_2 \leq 1\}$ as shown in Figure 4(b). Each periodic cell contains two masses, $m_a = m(1+\beta)$ and $m_b = m(1-\beta)$ with $-1 < \beta < 1$, connected by a spring of the length $\frac{a}{\sqrt{3}}$ and the spring constant k . Let \mathbf{b}_1 and \mathbf{b}_2 be the reciprocal lattice vectors given by $\mathbf{b}_1 = \frac{2\pi}{a} [1, -\frac{1}{\sqrt{3}}]$ and $\mathbf{b}_2 = \frac{2\pi}{a} [0, \frac{2}{\sqrt{3}}]$, which satisfy

$$\mathbf{a}_i \cdot \mathbf{b}_j = 2\pi\delta_{ij} = \begin{cases} 0, & i \neq j, \\ 2\pi, & i = j. \end{cases}$$

The hexagonal shape of the fundamental cell in the reciprocal lattices $\Lambda^* := \sum_{p,q \in \mathbb{Z}} p\mathbf{b}_1 + q\mathbf{b}_2$, or the Brillouin zone \mathbb{B} , is shown in Figure 5. Over the periodic cell $Y_{p,q}$, the displacements $U_{p,q}^a(t)$ and $U_{p,q}^b(t)$ for the masses a and b satisfy

$$\begin{aligned} m_a(U_{p,q}^a)'' + k(3U_{p,q}^a - U_{p,q}^b - U_{p-1,q}^b - U_{p,q-1}^b) &= 0, \\ m_b(U_{p,q}^b)'' + k(3U_{p,q}^b - U_{p,q}^a - U_{p+1,q}^a - U_{p,q+1}^a) &= 0. \end{aligned} \quad (19)$$

Consider the time-harmonic solution in the form of

$$U_{p,q}^a(t) = u_a \exp[i(\omega\tau + \boldsymbol{\kappa} \cdot \mathbf{r}_{p,q})] \quad \text{and} \quad U_{p,q}^b(t) = u_b \exp[i(\omega\tau + \boldsymbol{\kappa} \cdot \mathbf{r}_{p,q})], \quad (20)$$

where $\tau = \sqrt{k/mt}$ is nondimensional time scale, u_a and u_b are the amplitudes of displacements, the position vector $\mathbf{r}_{p,q} = p\mathbf{a}_1 + q\mathbf{a}_2$, the wave vector $\boldsymbol{\kappa} = \kappa_1\mathbf{b}_1 + \kappa_2\mathbf{b}_2$, and the wave frequency ω . Then u_a and u_b satisfy

$$\begin{aligned} (1+\beta)(-\omega^2)u_a + 3u_a + (-1 - e^{-i\boldsymbol{\kappa} \cdot \mathbf{a}_1} - e^{-i\boldsymbol{\kappa} \cdot \mathbf{a}_2})u_b &= 0, \\ (1-\beta)(-\omega^2)u_b + 3u_b + (-1 - e^{i\boldsymbol{\kappa} \cdot \mathbf{a}_1} - e^{i\boldsymbol{\kappa} \cdot \mathbf{a}_2})u_a &= 0, \end{aligned}$$

or equivalently,

$$M(\boldsymbol{\kappa})\mathbf{v}(\boldsymbol{\kappa}) = \omega^2\mathbf{v}(\boldsymbol{\kappa}), \quad (21)$$

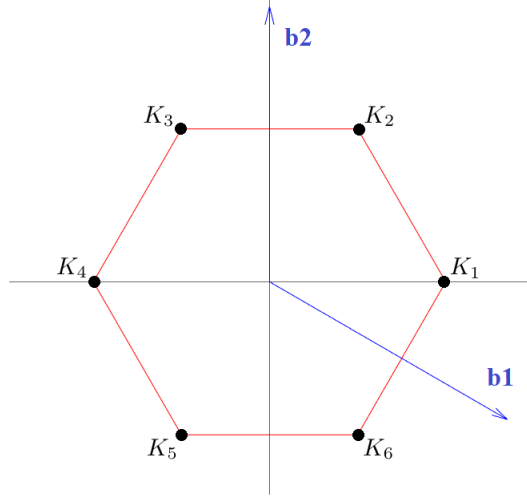


Figure 5: The Brillouin zone \mathbb{B} in the reciprocal lattice. The vertices of the Brillouin zone are $K_1 = \left(\frac{4\pi}{3a}, 0\right)$, $K_2 = \left(\frac{2\pi}{3a}, \frac{2\pi}{a\sqrt{3}}\right)$, $K_3 = \left(-\frac{2\pi}{3a}, \frac{2\pi}{a\sqrt{3}}\right)$, $K_4 = \left(-\frac{4\pi}{3a}, 0\right)$, $K_5 = \left(-\frac{2\pi}{3a}, -\frac{2\pi}{a\sqrt{3}}\right)$ and $K_6 = \left(\frac{2\pi}{3a}, -\frac{2\pi}{a\sqrt{3}}\right)$.

wherein

$$M(\boldsymbol{\kappa}) := \begin{bmatrix} \frac{3}{1+\beta} & \frac{\overline{d(\boldsymbol{\kappa})}}{1+\beta} \\ \frac{d(\boldsymbol{\kappa})}{1-\beta} & \frac{3}{1-\beta} \end{bmatrix} \quad \text{and} \quad \mathbf{v}(\boldsymbol{\kappa}) := \begin{bmatrix} u_a \\ u_b \end{bmatrix}. \quad (22)$$

In the above, $d(\boldsymbol{\kappa}) := -1 - e^{i\boldsymbol{\kappa} \cdot \mathbf{a}_1} - e^{i\boldsymbol{\kappa} \cdot \mathbf{a}_2} = -1 - e^{i2\pi\kappa_1} - e^{i2\pi\kappa_2}$ and $\overline{d(\boldsymbol{\kappa})}$ is the complex conjugate of $d(\boldsymbol{\kappa})$. The eigenvalues of the matrix $M(\boldsymbol{\kappa})$ are

$$\lambda_{\pm}(\boldsymbol{\kappa}) = \frac{3}{1-\beta^2} \pm \sqrt{\frac{9\beta^2}{(1-\beta^2)^2} + \frac{|d(\boldsymbol{\kappa})|^2}{1-\beta^2}}, \quad (23)$$

with the corresponding eigenvectors

$$\mathbf{v}_{\pm}(\boldsymbol{\kappa}) = \frac{1}{\chi(\boldsymbol{\kappa})} \begin{bmatrix} -\frac{\overline{d(\boldsymbol{\kappa})}}{3-\lambda_{\pm}(\boldsymbol{\kappa})(1+\beta)} \\ 1 \end{bmatrix}. \quad (24)$$

In the above, $\chi(\boldsymbol{\kappa})$ is a normalization constant such that

$$\mathbf{v}_{\pm}^*(\boldsymbol{\kappa}) \begin{bmatrix} 1+\beta & 0 \\ 0 & 1-\beta \end{bmatrix} \mathbf{v}_{\pm}(\boldsymbol{\kappa}) = 1, \quad (25)$$

where $\mathbf{v}_{\pm}^*(\boldsymbol{\kappa})$ is conjugate transpose of $\mathbf{v}_{\pm}(\boldsymbol{\kappa})$. In what follows, we use d , M , λ and \mathbf{v} instead of $d(\boldsymbol{\kappa})$, $M(\boldsymbol{\kappa})$, $\lambda(\boldsymbol{\kappa})$ and $\mathbf{v}(\boldsymbol{\kappa})$ for simplicity.

3.1.2 Dirac Point when $\beta = 0$

We first study the band structure when the two masses $m_a = m_b$, namely when $\beta = 0$. In particular, we show that Dirac point exists at the vertices of the Brillouin zone. A pair $(\boldsymbol{\kappa}^*, \lambda^*) \in \mathbb{B} \times \mathbb{R}$ is called a Dirac point (cf. [30], [31], [32], [33]) if

1. $\lambda_+(\boldsymbol{\kappa}^*) = \lambda_-(\boldsymbol{\kappa}^*) = \lambda^*$. In addition, there exist constants $\alpha > 0$ and $\gamma > 0$ such that the expansions

$$\begin{aligned} \lambda_+(\boldsymbol{\kappa}) &= \lambda^* + \alpha|\boldsymbol{\kappa} - \boldsymbol{\kappa}^*| + O(|\boldsymbol{\kappa}|^2), \\ \lambda_-(\boldsymbol{\kappa}) &= \lambda^* - \alpha|\boldsymbol{\kappa} - \boldsymbol{\kappa}^*| + O(|\boldsymbol{\kappa}|^2), \end{aligned}$$

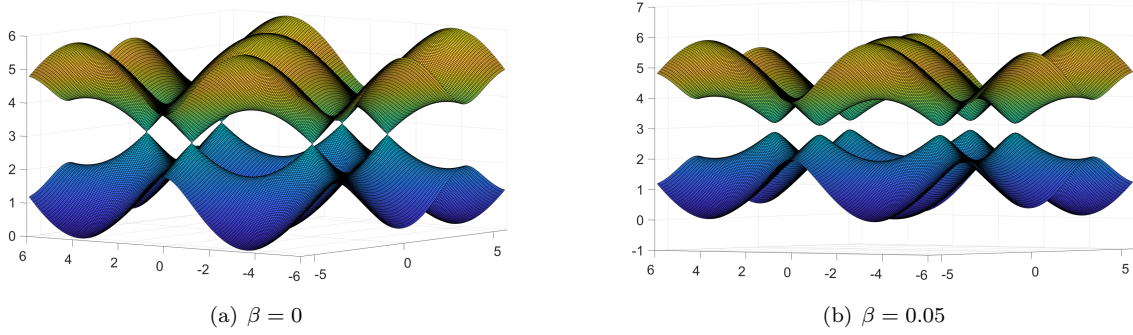


Figure 6: The band structure of the periodic system. (a) $\beta = 0$: The upper and lower bands touch at the vertices of Brillouin zone and form the Dirac points. (b) $\beta \neq 0$: A gap opens between the two bands.

hold for $|\boldsymbol{\kappa} - \boldsymbol{\kappa}^*| < \gamma$.

2. The eigenvalue $\lambda_{\pm}(\boldsymbol{\kappa})$ in (23) has multiplicity two when $\boldsymbol{\kappa} = \boldsymbol{\kappa}^*$.

Remark 1. Observe that if $\boldsymbol{\kappa}_i = K_i$, then $\boldsymbol{\kappa}_1 = \boldsymbol{\kappa}_3 + \mathbf{b}_1$, $\boldsymbol{\kappa}_3 = \boldsymbol{\kappa}_5 + \mathbf{b}_2$, $\boldsymbol{\kappa}_2 = \boldsymbol{\kappa}_6 + \mathbf{b}_2$ and $\boldsymbol{\kappa}_6 = \boldsymbol{\kappa}_4 + \mathbf{b}_1$. Therefore,

$$d(\boldsymbol{\kappa}_1) = d(\boldsymbol{\kappa}_3) = d(\boldsymbol{\kappa}_5) \quad \text{and} \quad d(\boldsymbol{\kappa}_2) = d(\boldsymbol{\kappa}_4) = d(\boldsymbol{\kappa}_6), \quad (26)$$

and it is sufficient to study the eigenvalues for $\boldsymbol{\kappa} = K_1$ and $\boldsymbol{\kappa} = K_4$.

When $\beta = 0$, from (23), the eigenvalues of M in (21) are

$$\lambda(\boldsymbol{\kappa}) = 3 \pm |d(\boldsymbol{\kappa})|.$$

Observe that

$$d(K_1) = -1 - \exp\left(ia \frac{4\pi}{3a}\right) - \exp\left(ia \frac{4\pi}{3a} + \frac{0\sqrt{3}}{2}\right) = 0.$$

We obtain $\lambda_+(K_1) = \lambda_-(K_1) = 3$ (Figure 6(a)). In addition, the derivative of $\lambda_+(\boldsymbol{\kappa})$ at $\boldsymbol{\kappa} = K_1$ along the direction $\mathbf{w} = (w_1, w_2)$ is

$$\begin{aligned} D_{\mathbf{w}}\lambda_+(K_1) &= \lim_{h \rightarrow 0^+} \frac{1}{h} \left[\lambda_+\left(\frac{4\pi}{3a} + w_1h, 0 + w_2h\right) - \lambda_+\left(\frac{4\pi}{3a}, 0\right) \right] \\ &= \lim_{h \rightarrow 0^+} \sqrt{\frac{1}{h^2} \left[4 \cos^2 \left[\frac{2\pi}{3} + \frac{w_1a}{2}h \right] + 4 \cos \left[\frac{2\pi}{3} + \frac{w_2a}{2}h \right] + 1 \right]} = \frac{a\sqrt{3}}{2}. \end{aligned}$$

Similarly,

$$D_{\mathbf{w}}\lambda_-(K_1) = -\frac{a\sqrt{3}}{2}.$$

Therefore, near K_1 , there holds

$$\lambda_{\pm}(\boldsymbol{\kappa}) = 3 \pm \frac{a\sqrt{3}}{2} |\boldsymbol{\kappa} - K_1| + O(|\boldsymbol{\kappa} - K_1|^2).$$

Following similar calculations, it can be shown that, for $\boldsymbol{\kappa}$ near K_4 ,

$$\lambda_{\pm}(\boldsymbol{\kappa}) = 3 \pm \frac{a\sqrt{3}}{2} |\boldsymbol{\kappa} - K_4| + O(|\boldsymbol{\kappa} - K_4|^2).$$

Note that have $M(\boldsymbol{\kappa}) = \begin{bmatrix} 3 & 0 \\ 0 & 3 \end{bmatrix}$ for $\boldsymbol{\kappa} = K_1, K_4$. Thus, the multiplicity of λ^* is 2. Therefore, $(K_i, 3)$ is a Dirac point for $i = 1, 4$.

Remark 2. When $\beta \neq 0$, we have $\lambda_-(\boldsymbol{\kappa}) < \lambda_+(\boldsymbol{\kappa})$ for $\boldsymbol{\kappa} \in \mathbb{B}$ and there is a gap between the upper and lower bands $\lambda_{\pm}(\boldsymbol{\kappa})$ in (24) which is called band gap.

3.1.3 Valley Chern Number

The Berry phase is a phase angle that describes the global phase change of a complex vector over a closed loop ν in its parameter space. The Berry phase associated with the band λ of the system in (21) is defined as a line integral around a closed loop ν in the Brillouin zone (cf. [29]);

$$\phi = \oint_{\nu} \mathbf{B}(\boldsymbol{\kappa}) d\boldsymbol{\kappa}. \quad (27)$$

In the above, $\mathbf{B}(\boldsymbol{\kappa}) = (A_{\kappa_x}(\boldsymbol{\kappa}), A_{\kappa_y}(\boldsymbol{\kappa}))$ is the Berry connection, wherein

$$A_j(\boldsymbol{\kappa}) := \langle \mathbf{v}(\boldsymbol{\kappa}), i\partial_j \mathbf{v}(\boldsymbol{\kappa}) \rangle, \quad j = \kappa_x, \kappa_y,$$

and \mathbf{v} is the eigenvector of M associated with the eigenvalue λ as defined in (24). By the Stokes' theorem,

$$\phi = \int_D \Omega(\boldsymbol{\kappa}) dS, \quad (28)$$

where D is the region enclosed by ν and $\Omega(\boldsymbol{\kappa})$ is Berry curvature given by $\Omega(\boldsymbol{\kappa}) = \partial_{\kappa_x} A_{\kappa_y}(\boldsymbol{\kappa}) - \partial_{\kappa_y} A_{\kappa_x}(\boldsymbol{\kappa})$. The valley Chern number for a Bloch wave vector $\boldsymbol{\kappa} = K$ is defined as Berry phase calculated over a closed loop ν containing K scaled by 2π (cf. [34]), i.e.,

$$C_{K,\nu} = \frac{1}{2\pi} \left(\oint_{\nu} \mathbf{B}(\boldsymbol{\kappa}) d\boldsymbol{\kappa} \pmod{2\pi} \right) = \frac{1}{2\pi} \int_D \Omega(\boldsymbol{\kappa}) dS. \quad (29)$$

Remark 3. For the eigenvector \mathbf{v} of the system in (21), a gauge transformation $\tilde{\mathbf{v}}(\boldsymbol{\kappa}) = e^{-i\varphi(\boldsymbol{\kappa})} \mathbf{v}(\boldsymbol{\kappa})$ for a differentiable function $\varphi(\boldsymbol{\kappa})$ gives that $\tilde{\mathbf{B}}(\boldsymbol{\kappa}) = \mathbf{B}(\boldsymbol{\kappa}) + \nabla\varphi(\boldsymbol{\kappa})$. Hence the Berry phase $\tilde{\phi} = \phi + 2\pi m$, for some $m \in \mathbb{Z}$, but $\tilde{\Omega}(\boldsymbol{\kappa}) = \Omega(\boldsymbol{\kappa})$ since $\nabla \times \nabla\varphi = 0$. As such (29) is defined with modulo 2π .

Let ν be a circle centered at K with radius $0 < r \ll 1$, we define the discrete valley Chern number as, for $N \in \mathbb{Z}^+$,

$$C_{K,\nu}^N = -\frac{1}{2\pi} \left[\text{Im} \left(\sum_{j=1}^N \log \langle \mathbf{v}(K + \boldsymbol{\kappa}_j), \mathbf{v}(K + \boldsymbol{\kappa}_{j+1}) \rangle \right) \pmod{2\pi} \right], \quad (30)$$

where $\boldsymbol{\kappa}_j = r(\cos(\theta_j), \sin(\theta_j))$, $\theta_j = -\pi + (j-1)\frac{2\pi}{N}$. It is clear that

$$C_{K,\nu} = \lim_{N \rightarrow \infty} C_{K,\nu}^N.$$

In what follows, we use C_K instead of $C_{K,\nu}$ for simplicity.

Lemma 3. For $N = 2n \in \mathbb{Z}^+$,

1. The Berry phase ϕ over the Brillouin zone is zero.
2. The valley Chern numbers for the vertices of Brillouin zone satisfy

$$C_{K_1}^N = C_{K_3}^N = C_{K_5}^N \quad \text{and} \quad C_{K_2}^N = C_{K_4}^N = C_{K_6}^N.$$

In addition, the valley Chern numbers satisfy $C_{K_1}^N = -C_{K_4}^N$.

3. Let \mathbf{v}_\pm be the eigenvectors of M defined in (24). If $\mathbf{v} = \mathbf{v}_+$, β and $C_{K_1}^N$ attain opposite signs, and if $\mathbf{v} = \mathbf{v}_-$, β and $C_{K_1}^N$ attain the same signs, where \mathbf{v}_\pm is the vector given in (24).

Proof. (i) For $N = 2n$ with $n \in \mathbb{Z}^+$, let $\{\hat{\boldsymbol{\kappa}}_j\}_{j=1}^N$ be equally spaced points on the boundary of Brillouin zone such that $\{K_1, K_2, \dots, K_6\} \subset \{\hat{\boldsymbol{\kappa}}_j\}_{j=1}^N$. Then, for $j = 1, 2, \dots, n+1$, we have

$$\hat{\boldsymbol{\kappa}}_j = -\hat{\boldsymbol{\kappa}}_{n+j},$$

which implies

$$d(\hat{\boldsymbol{\kappa}}_{j+n}) = \overline{d(\hat{\boldsymbol{\kappa}}_j)}$$

and thus

$$\mathbf{v}(\hat{\boldsymbol{\kappa}}_{j\pm n}) = \overline{\mathbf{v}(\hat{\boldsymbol{\kappa}}_j)}$$

for $1 \leq j \leq n+1$ in $\mathbf{v}(\hat{\boldsymbol{\kappa}}_{j+n})$ and for $n+2 \leq j \leq N$ in $\mathbf{v}(\hat{\boldsymbol{\kappa}}_{j-n})$. Thus we have

$$\begin{aligned} C^N &= -Im \left(\sum_{j=1}^N \log \langle \mathbf{v}(\hat{\boldsymbol{\kappa}}_j) | \mathbf{v}(\hat{\boldsymbol{\kappa}}_{j+1}) \rangle \right) \\ &= -Im \left(\sum_{j=1}^n \log \langle \mathbf{v}(\hat{\boldsymbol{\kappa}}_j) | \mathbf{v}(\hat{\boldsymbol{\kappa}}_{j+1}) \rangle + \sum_{j=n+1}^N \log \langle \mathbf{v}(\hat{\boldsymbol{\kappa}}_j) | \mathbf{v}(\hat{\boldsymbol{\kappa}}_{j+1}) \rangle \right) \\ &= -Im \left(\sum_{j=1}^n \log \langle \mathbf{v}(\hat{\boldsymbol{\kappa}}_{n+j})^* | \mathbf{v}(\hat{\boldsymbol{\kappa}}_{N/2+j+1})^* \rangle + \sum_{j=n+1}^N \log \langle \mathbf{v}(\hat{\boldsymbol{\kappa}}_j) | \mathbf{v}(\hat{\boldsymbol{\kappa}}_{j+1}) \rangle \right) \\ &= -Im \left(\sum_{n=n+1}^N \log \langle \mathbf{v}(\hat{\boldsymbol{\kappa}}_n)^* | \mathbf{v}(\hat{\boldsymbol{\kappa}}_{n+1})^* \rangle + \sum_{j=n+1}^N \log \langle \mathbf{v}(\hat{\boldsymbol{\kappa}}_j) | \mathbf{v}(\hat{\boldsymbol{\kappa}}_{j+1}) \rangle \right) \\ &= -Im \left(\sum_{n=n+1}^N \overline{\log \langle \mathbf{v}(\hat{\boldsymbol{\kappa}}_n) | \mathbf{v}(\hat{\boldsymbol{\kappa}}_{n+1}) \rangle} + \sum_{j=n+1}^N \log \langle \mathbf{v}(\hat{\boldsymbol{\kappa}}_j) | \mathbf{v}(\hat{\boldsymbol{\kappa}}_{j+1}) \rangle \right) \\ &= 0. \end{aligned}$$

(ii) By Remark 1, $d(K_1) = d(K_3) = d(K_5)$. Therefore, $\mathbf{v}(K_1) = \mathbf{v}(K_3) = \mathbf{v}(K_5)$ which implies $C_{K_1}^N = C_{K_3}^N = C_{K_5}^N$. Similarly, $C_{K_2}^N = C_{K_4}^N = C_{K_6}^N$. Let $\{\boldsymbol{\kappa}_j\}_{j=1}^N$ be the equally spaced points on the circle as given in the definition of the discrete valley Chern number, wherein $N = 2n$ for some $n \in \mathbb{Z}^+$. Note that $arg(\boldsymbol{\kappa}_{j+n}) = arg(\boldsymbol{\kappa}_j) + \pi$ for $j = 1, 2, \dots, n$, thus

$$K_4 + \boldsymbol{\kappa}_{j+n} = -(K_1 + \boldsymbol{\kappa}_j) \quad \text{for } 1 \leq j \leq n \quad \text{and} \quad K_4 + \boldsymbol{\kappa}_{j-n} = -(K_1 + \boldsymbol{\kappa}_j) \quad \text{for } n+1 \leq j \leq N. \quad (31)$$

Then,

$$d(K_4 + \boldsymbol{\kappa}_{j+n}) = \overline{d(K_1 + \boldsymbol{\kappa}_j)} \quad \text{and} \quad d(K_4 + \boldsymbol{\kappa}_{j-n}) = \overline{d(K_1 + \boldsymbol{\kappa}_j)},$$

which implies

$$\mathbf{v}(K_4 + \boldsymbol{\kappa}_{j\pm n}) = \overline{\mathbf{v}(K_1 + \boldsymbol{\kappa}_j)} \quad \text{for } 1 \leq j \leq n, \quad \text{and } n+1 \leq j \leq N.$$

Then

$$\begin{aligned}
C_4^N &= -Im \left(\sum_{j=1}^{2n} \log \langle \mathbf{v}(K_4 + \boldsymbol{\kappa}_j) | \mathbf{v}(K_4 + \boldsymbol{\kappa}_{j+1}) \rangle \right) \\
&= -Im \left(\sum_{j=1}^n \log \langle \mathbf{v}(K_4 + \boldsymbol{\kappa}_j) | \mathbf{v}(K_4 + \boldsymbol{\kappa}_{j+1}) \rangle + \sum_{j=n+1}^{2n} \log \langle \mathbf{v}(K_4 + \boldsymbol{\kappa}_j) | \mathbf{v}(K_4 + \boldsymbol{\kappa}_{j+1}) \rangle \right) \\
&= -Im \left(\sum_{m=n+1}^{2n} \log \langle \mathbf{v}(K_4 + \boldsymbol{\kappa}_{m-n}) | \mathbf{v}(K_4 + \boldsymbol{\kappa}_{m-n+1}) \rangle + \sum_{m=1}^n \log \langle \mathbf{v}(K_4 + \boldsymbol{\kappa}_{m+n}) | \mathbf{v}(K_4 + \boldsymbol{\kappa}_{m+n+1}) \rangle \right) \\
&= -Im \left(\sum_{m=n+1}^{2n} \log \langle \mathbf{v}^*(K_1 + \boldsymbol{\kappa}_m) | \mathbf{v}^*(K_1 + \boldsymbol{\kappa}_{m+1}) \rangle + \sum_{m=1}^n \log \langle \mathbf{v}^*(K_1 + \boldsymbol{\kappa}_m) | \mathbf{v}^*(K_1 + \boldsymbol{\kappa}_{m+1}) \rangle \right) \\
&= -Im \left(\left[\sum_{m=1}^{2n} \log \langle \mathbf{v}(K_1 + \boldsymbol{\kappa}_m) | \mathbf{v}(K_1 + \boldsymbol{\kappa}_{m+1}) \rangle \right]^* \right) = -C_1^N.
\end{aligned}$$

(iii) Let $\{\boldsymbol{\kappa}_j\}_{j=1}^N$ be as in (ii). Then we have

$$\langle \mathbf{v}(\boldsymbol{\kappa}_j) | \mathbf{v}(\boldsymbol{\kappa}_{j+1}) \rangle = (1 - \beta) |d(\boldsymbol{\kappa}_j)| |d(\boldsymbol{\kappa}_{j+1})| f_j(\beta) \left[r_j(\beta) e^{i(\xi_j - \xi_{j+1})} + 1 \right],$$

where

$$\begin{aligned}
f_j(\beta) &= \frac{\left(3\beta + \sqrt{9\beta^2 + (1 - \beta^2) |d(\boldsymbol{\kappa}_j)|^2} \right) \left(3\beta + \sqrt{9\beta^2 + (1 - \beta^2) |d(\boldsymbol{\kappa}_{j+1})|^2} \right)}{|d(\boldsymbol{\kappa}_j)| |d(\boldsymbol{\kappa}_{j+1})|}, \\
r_j(\beta) &= \frac{1 - \beta^2}{f_j(\beta)}, \quad \xi_j = \arg(d(\boldsymbol{\kappa}_j)).
\end{aligned}$$

For $\beta > 0$, $f_j(\beta) \in [1, \frac{36}{|d(\boldsymbol{\kappa}_j)| |d(\boldsymbol{\kappa}_{j+1})|}]$ is an increasing function of β and

$$\sqrt{1 - \beta^2} |d(\boldsymbol{\kappa}_j)| > 3\beta + \sqrt{9\beta^2 + (1 - \beta^2) |d(\boldsymbol{\kappa}_j)|^2},$$

thus $r_j(\beta) \in [0, 1]$. Consequently,

$$Im \left(\sum_{j=1}^N \log \langle \mathbf{v}(\boldsymbol{\kappa}_j), \mathbf{v}(\boldsymbol{\kappa}_{j+1}) \rangle \right) = Im \left(\sum_{j=1}^N \log \left(r_j(\beta) e^{i(\xi_j - \xi_{j+1})} + 1 \right) \right) = \sum_{j=1}^N \varepsilon_j, \quad (32)$$

where $\varepsilon_j \in \left(0, \frac{\xi_j - \xi_{j+1}}{2} \right)$ and we have used Lemma 1. Denoting $d(\boldsymbol{\kappa}(\theta))$ as $d(\theta)$, it follows that

$$d\left(-\frac{\pi}{3} - \tilde{\theta}\right) = \overline{d\left(-\frac{\pi}{3} + \tilde{\theta}\right)} \quad \text{and} \quad d\left(\frac{2\pi}{3} - \tilde{\theta}\right) = \overline{d\left(\frac{2\pi}{3} + \tilde{\theta}\right)},$$

for $\tilde{\theta} \in [0, \frac{2\pi}{3}]$ and $\tilde{\theta} \in [0, \frac{\pi}{3}]$ respectively. In addition, $d(-\pi/3)d(2\pi/3) < 0$. Therefore, as $\theta \in [-\pi, \pi]$, $d(\theta)$ surrounds the origin on the complex plane and $\arg(d(-\pi)) = \arg(d(\pi)) + 2\pi$. Then, by (32),

$$Im \left(\sum_{j=1}^N \log \langle \mathbf{v}(\boldsymbol{\kappa}_j), \mathbf{v}(\boldsymbol{\kappa}_{j+1}) \rangle \right) < \sum_{j=1}^N \frac{\xi_j - \xi_{j+1}}{2} = \frac{\xi_1 - \xi_{N+1}}{2} = \pi.$$

Therefore,

$$\text{Im} \left(\sum_{j=1}^N \log \langle \mathbf{v}(\boldsymbol{\kappa}_j), \mathbf{v}(\boldsymbol{\kappa}_{j+1}) \rangle \right) \in (0, \pi). \quad (33)$$

For $\beta < 0$, there holds $r_j(\beta) > 1$. By similar calculations, we obtain

$$\text{Im} \left(\sum_{j=1}^N \log \langle \mathbf{v}(\boldsymbol{\kappa}_j), \mathbf{v}(\boldsymbol{\kappa}_{j+1}) \rangle \right) \in (\pi, 3\pi). \quad (34)$$

The statement (iii) follows by (30), (33) and (34). \square

3.2 Edge Modes for the Topological Mechanical System

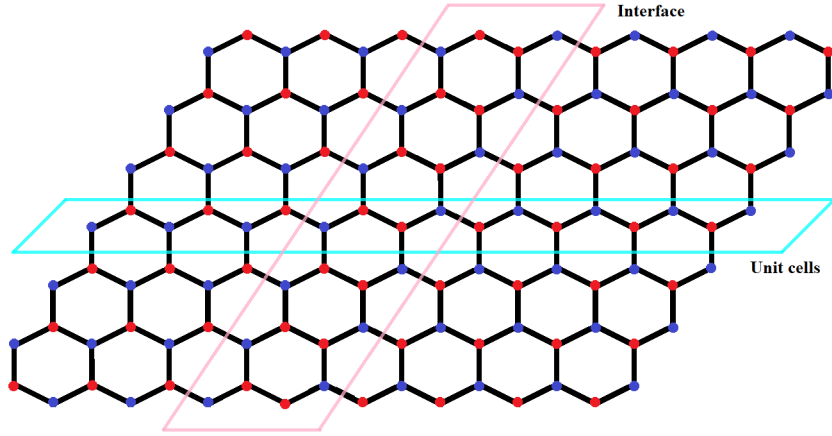


Figure 7: The topological mechanical system formed by two hexagonal lattices with opposite β values. The interface direction is parallel to \mathbf{a}_2 .

We consider a joint system formed by gluing two periodic hexagonal lattices with opposite β values. It forms an interface parallel to \mathbf{a}_2 where two identical masses are connected as shown in Figure 7. For $p \in \mathbb{Z}^+$ and $q \in \mathbb{Z}$, the governing equations for the displacements of the masses located at the left and right side of the interface are

$$\begin{aligned} m_a (U_{-p,q}^a)'' + k (U_{-p,q}^a - U_{-p,q}^b) - k (U_{-p,q}^a - U_{-(p-1),q}^b) - k (U_{-p,q}^a - U_{-p,q+1}^b) &= 0, \\ m_b (U_{-(p-1),q}^b)'' + k (U_{-(p-1),q}^b - U_{-(p-1),q-1}^a) - k (U_{-(p-1),q}^b - U_{-(p-1),q}^a) - k (U_{-(p-1),q}^b - U_{-p,q}^a) &= 0, \end{aligned} \quad (35)$$

and

$$\begin{aligned} m_a (U_{p,q}^a)'' + k (U_{p,q}^a - U_{p-1,q}^b) + k (U_{p,q}^a - U_{p,q-1}^b) + k (U_{p,q}^a - U_{p,q}^b) &= 0, \\ m_b (U_{p-1,q}^b)'' + k (U_{p-1,q}^b - U_{p-1,q}^a) + k (U_{p-1,q}^b - U_{p,q}^a) + k (U_{p-1,q}^b - U_{p-1,q+1}^a) &= 0, \end{aligned} \quad (36)$$

respectively. The governing equations for the displacement of the masses located at the interface are

$$\begin{aligned} m_a (U_{1,q}^a)'' + k (U_{1,q}^a - U_{-1,q}^a) + k (U_{1,q}^a - U_{1,q-1}^b) + k (U_{1,q}^a - U_{1,q}^b) &= 0, \\ m_a (U_{-1,q}^a)'' + k (U_{-1,q}^a - U_{1,q}^a) + k (U_{-1,q}^a - U_{-1,q+1}^b) + k (U_{-1,q}^a - U_{-1,q}^b) &= 0. \end{aligned} \quad (37)$$

For each $k_{||} \in [0, \frac{2\pi}{a}]$, we consider the solutions that propagate along the interface and decay along the horizontal direction by letting

$$U_{p,q}^a(t) = u_p^a e^{i\omega\gamma} e^{ik_{||}q} \quad \text{and} \quad U_{p,q}^b(t) = u_p^b e^{i\omega\gamma} e^{ik_{||}q}, \quad (38)$$

where $\gamma = \sqrt{k/mt}$. An edge mode $(U_{p,q}^a(t), U_{p,q}^b(t))$ is the nontrivial solution to (35) - (37) which decays to zero as $p \rightarrow \infty$.

We aim to show that there exist edge modes for the joint system in Figure 7 when $\beta \neq 0$. For each $k_{||} \in [0, \frac{2\pi}{a}]$, such edge mode attains an eigenfrequency $\omega(k_{||})$ such that $\omega^2(k_{||})$ located in the band gap $(\lambda_-(k_{||}), \lambda_+(k_{||}))$, where

$$\lambda_-(k_{||}) = \max_{\tilde{\mathbf{k}}} \lambda_-(\tilde{\mathbf{k}}) \quad \text{and} \quad \lambda_+(k_{||}) = \min_{\tilde{\mathbf{k}}} \lambda_+(\tilde{\mathbf{k}}).$$

In the above, $\tilde{\mathbf{k}} = k_{||}\mathbf{b}_1 + \frac{k_{||}a^2}{2\pi}\mathbf{b}_2$ and $k_{||} \in (0, 1)$.

Remark 4. For $k_{||} \in [0, \frac{2\pi}{a}]$, $\lambda_-(k_{||})$ and $\lambda_+(k_{||})$ occur when

$$\tilde{\mathbf{k}} = \left(\frac{n}{2} + \frac{k_{||}a^2}{4\pi} \right) \mathbf{b}_1 + \frac{k_{||}a^2}{2\pi} \mathbf{b}_2, \quad \text{for } n \in \{0, 1\},$$

with $(-1)^n \cos\left(\frac{k_{||}a^2}{2}\right) < 0$ and we have

$$\lambda_-(k_{||}) = \frac{3 - \sqrt{9\beta^2 + (1 - \beta^2)|d(\tilde{\mathbf{k}})|^2}}{1 - \beta^2} \quad \text{and} \quad \lambda_+(k_{||}) = \frac{3 + \sqrt{9\beta^2 + (1 - \beta^2)|d(\tilde{\mathbf{k}})|^2}}{1 - \beta^2}, \quad (39)$$

where $|d(\tilde{\mathbf{k}})| = \left| 1 + (-1)^n 2 \cos\left(\frac{k_{||}a^2}{2}\right) \right|$. It is clear that $\lambda_-(k_{||}) < \lambda_+(k_{||})$.

Our main result is stated in the following theorem.

Theorem 2. (Existence of edge mode) If two periodic systems with opposite β values are connected as in Figure 4(b), then for each $k_{||} \in [0, \frac{2\pi}{a}]$, there exists an edge mode $(U_{p,q}^a(t), U_{p,q}^b(t))$ in the form (38) with $\omega^2(k_{||}) \in (\lambda_-(k_{||}), \lambda_+(k_{||}))$.

Remark 5. By Lemma 3, if β_1 and β_2 attain opposite signs, then $C_{K_j}^{(1)} C_{K_j}^{(2)} < 0$ where $C_{K_j}^{(i)}$ is the valley Chern number calculated with β_i at K_j .

3.2.1 Transfer Matrix for the Periodic System

In this subsection, we compute the transfer matrices for the lattices on the left and right side of the interface. To simplify the calculations, we introduce the following notations:

$$\begin{aligned} \tau(k_{||}) &:= 3 - (1 + \beta)\omega^2(k_{||}), \\ \sigma(k_{||}) &:= 3 - (1 - \beta)\omega^2(k_{||}), \\ z(k_{||}) &:= 1 + e^{ik_{||}a^2}, \\ \xi(\sigma, k_{||}) &:= \tau\sigma - 1 - |z|^2, \end{aligned}$$

We consider the solutions in the form of (38) for (35)-(37). For the right periodic system, by (36), u_p^a and u_p^b satisfy

$$\begin{aligned} \tau u_p^a - u_{p-1}^b - u_p^b - u_p^b e^{-ik_{||}a^2} &= 0, \\ \sigma u_{p-1}^b - u_{p-1}^a - u_p^a - u_{p-1}^a e^{ik_{||}a^2} &= 0, \end{aligned} \quad (40)$$

which is reduced to $A(k_{||}) \mathbf{u}_{p-1} = B(k_{||}) \mathbf{u}_p$ where

$$A(k_{||}) = \begin{bmatrix} 0 & 1 \\ -z(k_{||}) & \sigma \end{bmatrix}, B(k_{||}) = \begin{bmatrix} \tau & -z(k_{||}) \\ 1 & 0 \end{bmatrix} \text{ and } \mathbf{u}_p = \begin{bmatrix} u_p^a \\ u_p^b \end{bmatrix} = \begin{bmatrix} u^a \\ u^b \end{bmatrix}_p.$$

We rewrite $A\mathbf{u}_{p-1} = B\mathbf{u}_p$ as

$$T_R(k_{||}) \mathbf{u}_{p-1} = \mathbf{u}_p,$$

where the transfer matrix

$$T_R(k_{||}) = B^{-1}A = \frac{1}{z} \begin{bmatrix} -|z|^2 & \bar{z}\sigma \\ -z\tau & \tau\sigma - 1 \end{bmatrix}.$$

The eigenpairs of T_R are

$$\lambda_{R,\pm}(k_{||}) = \frac{1}{2z} \left[\xi \pm \sqrt{\xi^2 - 4|z|^2} \right] \text{ and } \mathbf{v}_{R,\pm}(k_{||}) = \begin{bmatrix} \sigma \\ \lambda_{R,\pm} + z \end{bmatrix}.$$

Similarly, by (35), u_{-p}^a and u_{-p}^b satisfy

$$\begin{aligned} \tau u_{-p}^a - u_{-p}^b - u_{-(p-1)}^b - e^{ik_{||}a^2} u_{-p}^b &= 0, \\ \tau u_{-(p-1)}^b - u_{-(p-1)}^a - u_{-(p-1)}^a - e^{-ik_{||}a^2} u_{-p}^a &= 0. \end{aligned}$$

We obtain $T_L(k_{||}) \mathbf{u}_{-p} = \mathbf{u}_{-(p+1)}$, where the transfer matrix

$$T_L(k_{||}) = \frac{1}{z} \begin{bmatrix} -|z|^2 & z\sigma \\ -\bar{z}\tau & \tau\sigma - 1 \end{bmatrix}.$$

Since $T_R = \overline{T_L}$, the eigenpairs of T_L are

$$\lambda_{L,\pm}(k_{||}) = \overline{\lambda_{R,\pm}(k_{||})} = \frac{1}{2z} \left[\xi \pm \sqrt{\xi^2 - 4|z|^2} \right] \text{ and } \mathbf{v}_{L,\pm}(k_{||}) = \overline{\mathbf{v}_{R,\pm}(k_{||})} = \begin{bmatrix} \sigma \\ \lambda_{L,\pm} + \bar{z} \end{bmatrix}.$$

Remark 6. Along the interface, we have

$$|z|^2 = \left| 1 + e^{ik_{||}a^2} \right|^2 = \left((-1)^{n+1} 2 \cos\left(\frac{k_{||}a^2}{2}\right) \right)^2,$$

and $|d|^2 = (1 - |z|)^2$.

In order for \mathbf{u}_p to decay as $p \rightarrow \pm\infty$, it is necessary that $\mathbf{u}_1 = \begin{bmatrix} u^a \\ u^b \end{bmatrix}_1$ and $\mathbf{u}_{-1} = \begin{bmatrix} u^a \\ u^b \end{bmatrix}_{-1}$ are parallel to the eigenvectors of T_R and T_L whose corresponding eigenvalues have absolute value less than 1.

Remark 7. (i) If $\xi^2 - 4|z|^2 < 0$, then

$$|\lambda_R|^2 = |\lambda_L|^2 = \frac{1}{4|z|^2} \left| \xi \pm i\sqrt{4|z|^2 - \xi^2} \right|^2 = 1.$$

Since we consider $|\lambda_{L,R}| < 1$, there holds $\xi^2 - 4|z|^2 \geq 0$.

(ii) If $|\lambda_{R,+}|^2 < 1$, then

$$\xi \sqrt{\xi^2 - 4|z|^2} < 0,$$

which implies $\xi < 0$. If $|\lambda_{R,-}|^2 < 1$, then

$$-\xi \sqrt{\xi^2 - 4|z|^2} < 0,$$

which implies $\xi > 0$.

By Remark 7, the eigenvalue λ_R with $|\lambda_R| < 1$ is

$$\lambda_R = \begin{cases} \frac{1}{2\bar{z}} \left(\xi - \sqrt{\xi^2 - 4|z|^2} \right), & \text{for } \xi > 0, \\ \frac{1}{2\bar{z}} \left(\xi + \sqrt{\xi^2 - 4|z|^2} \right), & \text{for } \xi < 0. \end{cases} \quad (41)$$

Since $\lambda_{L,\pm} = \overline{\lambda_{R,\pm}}$, we have

$$\lambda_L = \begin{cases} \frac{1}{2z} \left(\xi - \sqrt{\xi^2 - 4|z|^2} \right), & \text{for } \xi > 0, \\ \frac{1}{2z} \left(\xi + \sqrt{\xi^2 - 4|z|^2} \right), & \text{for } \xi < 0. \end{cases} \quad (42)$$

Thus the parallelism condition above implies that

$$\begin{bmatrix} u_1^a \\ u_1^b \end{bmatrix} = c_1 \mathbf{v}_R = \begin{bmatrix} c_1 \sigma \\ c_1 (\lambda_R + z) \end{bmatrix} \quad \text{and} \quad \begin{bmatrix} u_{-1}^a \\ u_{-1}^b \end{bmatrix} = c_2 \mathbf{v}_L = \begin{bmatrix} c_2 \sigma \\ c_2 (\lambda_L + \bar{z}) \end{bmatrix}. \quad (43)$$

3.2.2 Proof of Theorem 2

By (37) and (38), we obtain

$$\begin{aligned} m_a(-\omega^2) \frac{k}{m} u_1^a e^{i\omega\tau} e^{ik|l|q} + k [u_1^a - u_{-1}^b] e^{i\omega\tau} e^{ik|l|q} + k [u_1^a - u_1^b] e^{i\omega\tau} e^{ik|l|q} + k [u_1^a - u_1^b e^{-ik|l|}] e^{i\omega\tau} e^{ik|l|q} &= 0, \\ m_a(-\omega^2) \frac{k}{m} u_{-1}^a e^{i\omega\tau} e^{ik|l|q} + k [u_{-1}^a - u_1^a] e^{i\omega\tau} e^{ik|l|q} + k [u_{-1}^a - u_{-1}^b] e^{i\omega\tau} e^{ik|l|q} + k [u_{-1}^a - u_{-1}^b e^{ik|l|}] e^{i\omega\tau} e^{ik|l|q} &= 0, \end{aligned}$$

which implies

$$\begin{aligned} \tau u_1^a - u_{-1}^a - \bar{z} u_1^b &= 0, \\ \tau u_{-1}^a - u_1^a - z u_{-1}^b &= 0. \end{aligned} \quad (44)$$

Then (44) can be simplified as

$$\begin{aligned} \tau c_1 \sigma - \bar{z} c_1 (\lambda_R z) - c_2 \sigma &= 0, \\ \tau c_2 \sigma - z c_2 (\lambda_L \bar{z}) - c_1 \sigma &= 0. \end{aligned} \quad (45)$$

For $\sigma = 0$, the first equation in (45) implies that

$$c_1 \lambda_R |z|^2 = 0.$$

which is equivalent to $c_1 = 0$ and it gives the trivial solution for (40). The first equation in (45) implies that, for $\sigma \neq 0$,

$$c_2 = \frac{1}{\sigma} c_1 (\tau \sigma - \bar{z} (\lambda_R + z)), \quad (46)$$

(46) and the second equation in (45) together imply that

$$c_1 \sigma = \frac{1}{\sigma} c_1 (\tau \sigma - \bar{z} (\lambda_R + z)) (\tau \sigma - z (\lambda_L + \bar{z})),$$

which is equivalent to

$$4\sigma^2 = \begin{cases} \left| \xi + 2 - \sqrt{\xi^2 - 4|z|^2} \right|^2, & \text{for } \xi < 0, \\ \left| \xi + 2 + \sqrt{\xi^2 - 4|z|^2} \right|^2, & \text{for } \xi > 0, \end{cases} \quad (47)$$

by (41). We consider $\xi < 0$ and $\xi > 0$ respectively to obtain a solution to (47). We have, if $\xi < 0$,

$$2\sigma = \xi + 2 - \sqrt{\xi^2 - 4|z|^2} \text{ or } 2\sigma = -(\xi + 2) + \sqrt{\xi^2 - 4|z|^2}.$$

(i) If $2\sigma = \xi + 2 - \sqrt{\xi^2 - 4|z|^2}$, then

$$4\sigma^2 - 4\sigma(\xi + 2) + \xi^2 + 4\xi + 4 = \xi^2 - 4|z|^2,$$

which implies

$$-\frac{1+\beta}{1-\beta}\sigma^3 + \left[1 + \frac{6\beta}{1-\beta} + \frac{6\beta}{1-\beta}\right]\sigma^2 - \sigma \left[1 - |z|^2 + \frac{6\beta}{1-\beta}\right] = 0. \quad (48)$$

The above equation attains two nonzero roots:

$$\sigma_1 = \frac{1 + 3\beta - \sqrt{4\beta^2 + (1 - \beta^2)|z|^2}}{(1 + \beta)}, \quad \sigma_2 = \frac{1 + 3\beta + \sqrt{4\beta^2 + (1 - \beta^2)|z|^2}}{(1 + \beta)}.$$

Note that, for $\beta \in (-1, 1)$,

$$0 > \xi(\sigma_2, k_{||}) \geq 4 \frac{|\beta| - \beta^2}{1 - \beta^2} > 0,$$

which is a contradiction to $\xi < 0$. For σ_1 ,

$$\xi(\sigma_1, k_{||}) = \frac{1 + \beta}{1 - \beta}\sigma^2 - \frac{6\beta}{1 - \beta}\sigma - |z|^2 - 1 = -\frac{4\beta^2 + 2\sqrt{4\beta^2 + (1 - \beta^2)|z|^2}}{1 - \beta^2} < 0.$$

Therefore,

$$\tilde{\sigma}_1 = \frac{1 + 3\beta - \sqrt{4\beta^2 + (1 - \beta^2)|z|^2}}{(1 + \beta)}$$

is one root of (48).

(ii) If $2\sigma = -(\xi + 2) + \sqrt{\xi^2 - 4|z|^2}$, by similar calculations, we obtain two more roots

$$\sigma_3 = \frac{-1 + 3\beta + \sqrt{16\beta^2 + (1 - \beta^2)|z|^2}}{1 + \beta}, \text{ and } \sigma_4 = \frac{-1 + 3\beta - \sqrt{16\beta^2 + (1 - \beta^2)|z|^2}}{1 + \beta}.$$

Similarly, we have

$$0 > \xi(\sigma_4, k_{||}) = 2 \frac{4\beta^2 + 4|\beta|}{1 - \beta^2} \geq 0,$$

$$\xi(\sigma_3, k_{||}) = \frac{8\beta^2 - 2\sqrt{16\beta^2 + (1 - \beta^2)|z|^2}}{1 - \beta^2} \leq 8 \frac{\beta^2 - |\beta|}{1 - \beta^2} \leq 0.$$

Thus, we obtain

$$\tilde{\sigma}_2 = \frac{-1 + 3\beta + \sqrt{16\beta^2 + (1 - \beta^2)|z|^2}}{1 + \beta},$$

as another root of (47).

By similar calculations for $\xi > 0$, we obtain two more roots:

$$\tilde{\sigma}_3 = \frac{1 + 3\beta + \sqrt{4\beta^2 + (1 - \beta^2)|z|^2}}{1 + \beta} \quad \text{and} \quad \tilde{\sigma}_4 = \frac{-1 + 3\beta - \sqrt{16\beta^2 + (1 - \beta^2)|z|^2}}{1 + \beta}.$$

From the relation $\sigma = 3 - (1 + \beta)\omega^2$, we obtain the corresponding eigenvalues:

$$\begin{aligned} \omega_1^2(k_{||}) &= \frac{2 + \sqrt{4\beta^2 + (1 - \beta^2)|z|^2}}{1 - \beta^2}, \\ \omega_2^2(k_{||}) &= \frac{4 - \sqrt{16\beta^2 + (1 - \beta^2)|z|^2}}{1 - \beta^2}, \\ \omega_3^2(k_{||}) &= \frac{2 - \sqrt{4\beta^2 + (1 - \beta^2)|z|^2}}{1 - \beta^2}, \\ \omega_4^2(k_{||}) &= \frac{4 + \sqrt{16\beta^2 + (1 - \beta^2)|z|^2}}{1 - \beta^2}. \end{aligned} \tag{49}$$

Next we show that $\omega_j^2(k_{||}) \in (\lambda_-(k_{||}), \lambda_+(k_{||}))$ for $j = 1, 2$ but $\omega_j^2(k_{||}) \notin (\lambda_-(k_{||}), \lambda_+(k_{||}))$ for $j = 3, 4$. For $\omega_1^2(k_{||})$, we have

$$\begin{aligned} w_1^2 - \lambda_- &= \frac{2 + \sqrt{4\beta^2 + (1 - \beta^2)|z|^2}}{1 - \beta^2} - \frac{3 - \sqrt{9\beta^2 + (1 - \beta^2)|d|^2}}{1 - \beta^2} \\ &\geq \frac{1}{1 - \beta^2} \left[-1 + \sqrt{1 + 2[4\beta^2 + (1 - \beta^2)|z|^2]} \right] \geq 0. \end{aligned}$$

In the above, we have used Remark (6) to relate z and d . Thus, $\omega_1^2 \geq \lambda_-$. Similarly,

$$\begin{aligned} w_1^2 - \lambda_+ &= \frac{2 + \sqrt{4\beta^2 + (1 - \beta^2)|z|^2}}{1 - \beta^2} - \frac{3 + \sqrt{9\beta^2 + (1 - \beta^2)|d|^2}}{1 - \beta^2} \\ &\leq \frac{1}{1 - \beta^2} \left[\sqrt{4\beta^2 + (1 - \beta^2)|z|^2} - 1 - \sqrt{4\beta^2 + (1 - \beta^2)|z|^2 + 4} \right] \leq 0. \end{aligned}$$

Thus, $\omega_1^2 \leq \lambda_+$ and we have $\omega_1^2 \in [\lambda_-, \lambda_+]$. By similar calculations, we can show $\omega_2^2 \in [\lambda_-, \lambda_+]$. However, if $\omega_3^2 \geq \lambda_-$, then

$$\frac{2 - \sqrt{4\beta^2 + (1 - \beta^2)|z|^2}}{1 - \beta^2} \geq \frac{3 - \sqrt{9\beta^2 + (1 - \beta^2)|d|^2}}{1 - \beta^2},$$

which can be simplified as

$$-\beta^2(1 - \beta^2)(|z| - 2)^2 \geq 0,$$

which is impossible. Thus, $\omega_3^2 < \lambda_-$ and $\omega_3^2 \notin [\lambda_-, \lambda_+]$. Similarly, we can show $\omega_4^2 > \lambda_+$ and $\omega_4^2 \notin [\lambda_-, \lambda_+]$. Figure 8 shows that $\omega_1^2(k_{||})$ and $\omega_2^2(k_{||})$ located in the band gap $(\lambda_-(k_{||}), \lambda_+(k_{||}))$ when $a = 1$ and $\beta = 0.1$.

Acknowledgements

The work of R. Ozdemir and J. Lin is partially supported the NSF grant DMS-2011148.

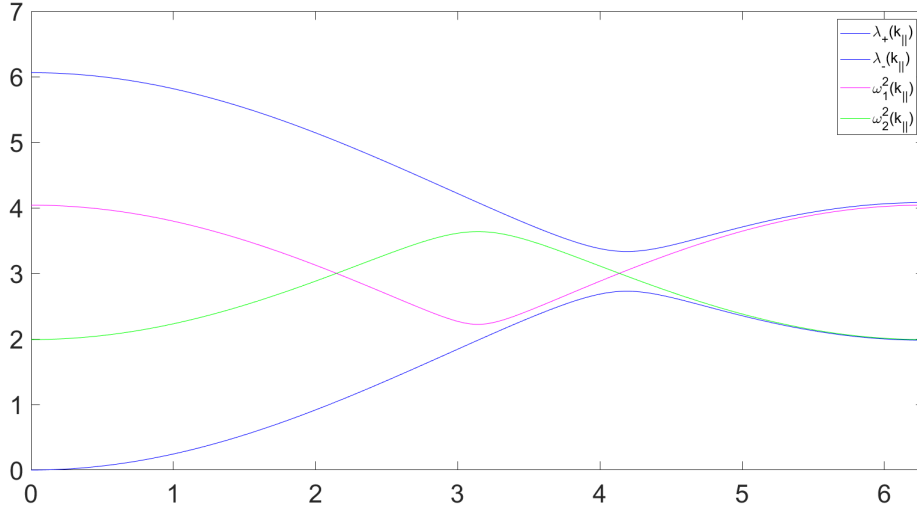


Figure 8: The upper and lower bands $\lambda_{\pm}(k_{||})$, and the eigenvalues of the edge modes, $\omega_1^2(k_{||})$ and $\omega_2^2(k_{||})$, when $a = 1$ and $\beta = 0.1$.

References

- [1] C. L. Kane, “Topological band theory and the \mathbb{Z}_2 invariant,” in *Contemporary Concepts of Condensed Matter Science*, vol. 6, pp. 3–34, Elsevier, 2013.
- [2] S. Raghu and F. D. M. Haldane, “Analogues of quantum-hall-effect edge states in photonic crystals,” *Physical Review A*, vol. 78, no. 3, p. 033834, 2008.
- [3] A. B. Khanikaev, S. Hossein Mousavi, W.-K. Tse, M. Kargarian, A. H. MacDonald, and G. Shvets, “Photonic topological insulators,” *Nature materials*, vol. 12, no. 3, pp. 233–239, 2013.
- [4] L. Lu, J. D. Joannopoulos, and M. Soljačić, “Topological photonics,” *Nature photonics*, vol. 8, no. 11, pp. 821–829, 2014.
- [5] G. Ma, M. Xiao, and C. T. Chan, “Topological phases in acoustic and mechanical systems,” *Nature Reviews Physics*, vol. 1, no. 4, pp. 281–294, 2019.
- [6] T. Ozawa, H. M. Price, A. Amo, N. Goldman, M. Hafezi, L. Lu, M. C. Rechtsman, D. Schuster, J. Simon, O. Zilberberg, *et al.*, “Topological photonics,” *Reviews of Modern Physics*, vol. 91, no. 1, p. 015006, 2019.
- [7] M. Xiao, G. Ma, Z. Yang, P. Sheng, Z. Zhang, and C. T. Chan, “Geometric phase and band inversion in periodic acoustic systems,” *Nature Physics*, vol. 11, no. 3, pp. 240–244, 2015.
- [8] A. B. Khanikaev, R. Fleury, S. H. Mousavi, and A. Alu, “Topologically robust sound propagation in an angular-momentum-biased graphene-like resonator lattice,” *Nature communications*, vol. 6, no. 1, p. 8260, 2015.
- [9] L. M. Nash, D. Kleckner, A. Read, V. Vitelli, A. M. Turner, and W. T. Irvine, “Topological mechanics of gyroscopic metamaterials,” *Proceedings of the National Academy of Sciences*, vol. 112, no. 47, pp. 14495–14500, 2015.
- [10] Z. Wang, Y. Chong, J. D. Joannopoulos, and M. Soljačić, “Observation of unidirectional backscattering-immune topological electromagnetic states,” *Nature*, vol. 461, no. 7265, pp. 772–775, 2009.

- [11] J. Lu, C. Qiu, M. Ke, and Z. Liu, “Valley vortex states in sonic crystals,” *Physical review letters*, vol. 116, no. 9, p. 093901, 2016.
- [12] L. Ye, C. Qiu, J. Lu, X. Wen, Y. Shen, M. Ke, F. Zhang, and Z. Liu, “Observation of acoustic valley vortex states and valley-chirality locked beam splitting,” *Physical Review B*, vol. 95, no. 17, p. 174106, 2017.
- [13] T. Ma and G. Shvets, “All-si valley-hall photonic topological insulator,” *New Journal of Physics*, vol. 18, no. 2, p. 025012, 2016.
- [14] L.-H. Wu and X. Hu, “Scheme for achieving a topological photonic crystal by using dielectric material,” *Physical review letters*, vol. 114, no. 22, p. 223901, 2015.
- [15] R. K. Pal, J. Vila, and M. Ruzzene, “Topologically protected edge states in mechanical metamaterials,” *Advances in Applied Mechanics*, vol. 52, pp. 147–181, 2019.
- [16] X. Zheng, J. Zhao, N. Kacem, and P. Liu, “Toward acceleration sensing based on topological gyroscopic metamaterials,” *Physical Review B*, vol. 106, no. 9, p. 094307, 2022.
- [17] H. Ammari, B. Davies, E. O. Hiltunen, and S. Yu, “Topologically protected edge modes in one-dimensional chains of subwavelength resonators,” *Journal de Mathématiques Pures et Appliquées*, vol. 144, pp. 17–49, 2020.
- [18] H. Ammari, B. Davies, and E. O. Hiltunen, “Robust edge modes in dislocated systems of subwavelength resonators,” *Journal of the London Mathematical Society*, vol. 106, no. 3, pp. 2075–2135, 2022.
- [19] A. Drouot and M. I. Weinstein, “Edge states and the valley hall effect,” *Advances in Mathematics*, vol. 368, p. 107142, 2020.
- [20] C. L. Fefferman, J. P. Lee-Thorp, and M. I. Weinstein, “Edge states in honeycomb structures,” *Annals of PDE*, vol. 2, pp. 1–80, 2016.
- [21] C. L. Fefferman, J. P. Lee-Thorp, and M. I. Weinstein, “Topologically protected states in one-dimensional continuous systems and dirac points,” *Proceedings of the National Academy of Sciences*, vol. 111, no. 24, pp. 8759–8763, 2014.
- [22] J. Qiu, J. Lin, P. Xie, and H. Zhang, “Mathematical theory for the interface mode in a waveguide bifurcated from a dirac point,” *arXiv preprint arXiv:2304.10843*, 2023.
- [23] Z. Zhang, P. Delplace, and R. Fleury, “Superior robustness of anomalous non-reciprocal topological edge states,” *Nature*, vol. 598, no. 7880, pp. 293–297, 2021.
- [24] G. Bal, “Topological protection of perturbed edge states,” *arXiv preprint arXiv:1709.00605*, 2017.
- [25] G. Bal, “Continuous bulk and interface description of topological insulators,” *Journal of Mathematical Physics*, vol. 60, no. 8, 2019.
- [26] A. Drouot, “Microlocal analysis of the bulk-edge correspondence,” *Communications in Mathematical Physics*, vol. 383, pp. 2069–2112, 2021.
- [27] P. Elbau and G.-M. Graf, “Equality of bulk and edge hall conductance revisited,” *Communications in mathematical physics*, vol. 229, pp. 415–432, 2002.
- [28] A. Elgart, G. Graf, and J. Schenker, “Equality of the bulk and edge hall conductances in a mobility gap,” *Communications in mathematical physics*, vol. 259, pp. 185–221, 2005.
- [29] D. Vanderbilt, *Berry phases in electronic structure theory: electric polarization, orbital magnetization and topological insulators*. Cambridge University Press, 2018.

- [30] J. Lin and H. Zhang, “Mathematical theory for topological photonic materials in one dimension,” *Journal of Physics A: Mathematical and Theoretical*, vol. 55, p. 495203, dec 2022.
- [31] J. P. Lee-Thorp, M. I. Weinstein, and Y. Zhu, “Elliptic operators with honeycomb symmetry: Dirac points, edge states and applications to photonic graphene,” *Archive for Rational Mechanics and Analysis*, vol. 232, pp. 1–63, 2019.
- [32] C. L. Fefferman, J. P. Lee-Thorp, and M. I. Weinstein, “Honeycomb schrödinger operators in the strong binding regime,” *Communications on Pure and Applied Mathematics*, vol. 71, no. 6, pp. 1178–1270, 2018.
- [33] C. L. Fefferman and M. I. Weinstein, “Wave packets in honeycomb structures and two-dimensional dirac equations,” *Communications in Mathematical Physics*, vol. 326, pp. 251–286, 2014.
- [34] D. Xiao, W. Yao, and Q. Niu, “Valley-contrasting physics in graphene: magnetic moment and topological transport,” *Physical review letters*, vol. 99, no. 23, p. 236809, 2007.